Environ Sci Pollut Res (2016) 23:4844–4858
DOI 10.1007/s11356-015-5683-0

RESEARCH ARTICLE

Surface capping and size-dependent toxicity of gold nanoparticles on different trophic levels

V. Iswarya[1] · J. Manivannan[2] · Arpita De[2] · Subhabrata Paul[2] · Rajdeep Roy[1] · J. B. Johnson[1] · Rita Kundu[2] · N. Chandrasekaran[1] · Anita Mukherjee[2] · Amitava Mukherjee[1]

Received: 8 May 2015 / Accepted: 22 October 2015 / Published online: 6 November 2015

Abstract In the present study, the toxicity of gold nanoparticles (Au NPs) was evaluated on various trophic organisms. Bacteria, algae, cell line, and mice were used as models representing different trophic levels. Two different sizes (CIT_{30} and CIT_{40}) and surface-capped (CIT_{30}–polyvinyl pyrrolidone (PVP)-capped) Au NPs were selected. CIT_{30} Au NP aggregated more rapidly than CIT_{40} Au NP, while an additional capping of PVP (CIT_{30}–PVP capped Au NP) was found to enhance its stability in sterile lake water medium. Interestingly, all the forms of NPs evaluated were stable in the cell culture medium during the exposure period. Size- and dose-dependent cytotoxicities were observed in both bacteria and algae, with a strong dependence on reactive oxygen species (ROS) generation and lactate dehydrogenase (LDH) release. CIT_{30}–PVP capped Au NP showed a significant decrease in toxicity compared to CIT_{30} Au NP in bacteria and algae. In the SiHa cell line, dose- and exposure-dependent decline in cell viability were noted for all three types of Au NPs. In mice, the induction of DNA damage was size and dose dependent, and surface functionalization with PVP reduced the toxic effects of CIT_{30} Au NP. The exposure to CIT_{30}, CIT_{40}, and CIT_{30}–PVP capped Au NPs caused an alteration of the oxidative stress-related endpoints in mice hepatocytes. The toxic effects of the gold nanoparticles were found to vary in diverse test systems, accentuating the importance of size and surface functionalization at different trophic levels.

Keywords Au NPs · Size dependent · Surface capping · Ecotoxicity · Genotoxicity · Stability

Responsible editor: Philippe Garrigues

V. Iswarya and Arpita De contributed equally to this work.

Electronic supplementary material The online version of this article (doi:10.1007/s11356-015-5683-0) contains supplementary material, which is available to authorized users.

✉ Anita Mukherjee
prof.amukherjee.cu@gmail.com

✉ Amitava Mukherjee
amit.mookerjea@gmail.com; amitav@vit.ac.in

[1] Centre for Nanobiotechnology, VIT University, Vellore 632014, India

[2] Cell Biology and Genetic Toxicology Lab, Centre of Advanced Study, Department of Botany, University of Calcutta, Kolkata 700019, India

Introduction

Gold nanoparticles (Au NPs) are used in different applications such as commercial products (Eustis and El-Sayed 2006), diagnostics and therapeutics (Sokolov et al. 2003), chemical and biological sensing (Anker et al. 2008), drug delivery (Jain et al. 2007), cancer treatment (Wu et al. 2011), and immunoassays (Alkilany and Murphy 2010). It is estimated that global investment in gold has reached about US$12 billion in 2015 (Keel et al. 2010). Due to their increased usage, discharge of Au NPs (from the products and effluents) into the environment will impose a hazard to the aquatic ecosystem and also to the other organisms.

Microorganisms form the base of the food web, which helps in the maintenance of the ecosystem as a producer and also a decomposer (Schaechter et al. 2006; Osler and Sommerkorn 2007). The toxicity of Au NPs on *Pseudomonas flourescens* differed depending on the surface capping agents. Polyvinyl pyrrolidone (PVP)-capped Au NPs showed a measurable toxic effect than citrate-capped Au NPs (Nur 2013).

As a primary producer, algae help in the maintenance of the aquatic food web (Aruoja et al. 2009). Hoecke et al. (2013) reported the eco-toxic effect of two types of polymer-coated gold NPs on algal species (*Pseudokirchneriella subcapitata*). A recent report on *Chlamydomonas reinharditii* highlighted the importance of surface capping on the toxicity of Au NPs (Behra et al. 2015).

Chuang et al. (2013) studied the cytotoxic effects of gold nanoparticles in five different types of mammalian cell lines such as AGS (human gastric adenocarcinoma cells), A549 (human lung adenocarcinoma epithelial), NIH3T3 (mouse embryonic fibroblast), PK-15 (porcine kidney), and Vero (African green monkey kidney). Biologically synthesized Au NPs exhibited lower toxicity on A549 cells than chemically synthesized Au NPs (Sathishkumar et al. 2014). Literature is replete with reports on the size- and shape-dependent toxic effects of gold nanoparticles in different cell lines (Chueh et al. 2014; Coradeghini et al. 2013) and murine models (Schulz et al. 2012). The results of Au NP toxicity are often conflicting in nature since different investigators use different cell lines, diverse sizes of nanoparticles, special surface groups, different doses, and different sampling points.

Reports also suggest that the in vivo toxic effect of nanoparticles is different from that of an in vitro study (Schipper et al. 2008; Sayes et al. 2007). Sayes et al. (2007) compared the in vitro and in vivo toxicity effects of nano-fullerenes (C_{60} and $C_{60}(OH)_{24}$) on the lung tissues of rats and found them to be distinct. Therefore, it is necessary to study the in vivo toxicity of Au NPs. Yang et al. (2014) examined the in vivo toxic effects of Au NPs based on the nanoparticle size and gestational age. Zhang et al. (2011) reported the size-dependent (5, 10, 30, and 60 nm) in vivo toxicity of PEG-coated gold nanoparticles in mice. A genotoxic effect of different sizes of gold nanoparticles was observed by Schulz et al. (2012) in the lungs of rats. Yah (2013) discussed various in vivo and in vitro toxicity effects of gold nanoparticles in relation to their physiochemical properties.

In the absence of comprehensive prior reports, a study was warranted for Au NP toxicity across trophic levels using various model organisms. The purpose of the current study was to assess the in vitro and in vivo toxicity of Au NPs, on different trophic organisms, affected by their size and surface functionalization. To investigate the size effect of Au NPs, two different sizes of citrate-capped Au NPs (CIT_{30} and CIT_{40}) were selected and compared in this study. Since CIT_{30} was found to be the more potent toxicant between the two, it was modified with the polymer polyvinyl pyrrolidone (PVP) to make the Au NP less toxic as well as determine the toxicity of the PVP coating alone, if any. The toxicity of Au NPs at different trophic levels was assessed using freshwater bacteria, *Bacillus aquimaris*; freshwater green algae, *Chlorella* sp.; a human SiHa cell line, and a mice model.

Materials and methods

Chemicals

Tetra aurochloric acid ($HAuCl_4$), trisodium citrate, and polyvinylpyrrolidone (PVP, K-30) were purchased from Sisco Research Laboratories Pvt Ltd (Mumbai, India). BG-11 broth; nicotinamide adenine dinucleotide, reduced (β-NADH); and Eagle's minimal essential medium (Eagle's MEM) were procured from Himedia Labs Pvt Ltd (Mumbai, India). 2′,7′-Dichlorofluorescin diacetate (DCFH-DA), MTT, and sodium pyruvate were obtained from Sigma-Aldrich (St. Louis, MO, USA). All the other chemicals used were of analytical grade.

Synthesis of Au NPs

Citrate-capped gold nanoparticles (Au NPs) of two different sizes (30 and 40 nm; herein referred to as CIT_{30} and CIT_{40}, respectively) and one polyvinyl pyrrolidone (PVP)-capped Au NP (herein referred to as CIT_{30}–PVP capped) were prepared and further used for the toxicity assessment of Au NPs in various organisms.

CIT_{30} Au NPs CIT_{30} Au NPs were synthesized by following the standard Turkevich protocol with minor modifications (Turkevich et al. 1953; Rohiman et al. 2011). 23.75 mL of Milli-Q water was heated in a round-bottom flask until the temperature reached 90 °C. One milliliter of 136 mM trisodium citrate and 250 μL of 25.4 mM tetra aurochloric acid were added to the solution under continuous stirring condition. Then, the solution was further heated for about 10 min till a wine-red color was obtained which indicates the formation of Au NPs. The synthesized Au nanoparticle solution was allowed to cool at room temperature and stored at 4 °C.

CIT_{40} Au NPs CIT_{40} Au nanoparticles were obtained by a Turkevich method (Turkevich et al. 1953) with slight modification as per the procedure followed by Kumar et al. (2006). 0.25 mM tetra aurochloric acid was added to 25 mL of Milli-Q water, which was previously heated at 90 °C on a hot plate in a stirring condition. Then, 250 μL of 30.4 mM trisodium citrate was added quickly to the reaction mixture. An immediate color change from yellow to wine red was obtained within 10 min. The solution was further allowed to continue the reaction at the same boiling point for about 15 min to ensure that the reaction is fully completed. Then, the solution was allowed to cool to room temperature and stored at 4 °C.

CIT_{30}–PVP capped Au NPs PVP-capped Au NPs (CIT_{30}–PVP capped) were prepared by coating PVP (1.25 mM) on the surface of CIT_{30} Au NPs. After the synthesis of CIT_{30} Au NPs (red color formation), 1 mL of 1.25 mM PVP was added and

the solution was stirred for 30 min, allowed to cool to room temperature, and stored at 4 °C.

Characterization of Au NPs

The primary size and shape of the synthesized Au NPs were examined using transmission electron microscopy (TEM, FEI Tecnai T20 S-TWIN TEM). The hydrodynamic size of the Au NPs was analyzed by dynamic light scattering analysis (DLS, 90 Plus Particle Size Analyzer, Brookhaven Instruments Corp., USA). Similarly, the hydrodynamic size distribution of Au NPs (1 mg/L of CIT_{30}, CIT_{40}, and CIT_{30}–PVP capped) in sterile filtered lake water and cell culture media (Eagle's MEM) was evaluated to determine the stability of Au NPs in their respective matrices at different time intervals (0, 6, 12, and 24 h) by DLS.

Toxicity of Au NPs towards lower organisms

Toxicity assessment of Au NPs on bacteria

Test organism The bacterial strain *B. aquimaris*, a gram-variable bacterium isolated from VIT lake at VIT University, Vellore Campus, Tamil Nadu (as detailed in our previous report, Kumar et al. 2014), was used as a test organism. The toxicity experiments were carried out in sterile filtered lake water as a freshwater matrix. Lake water collected from VIT Lake was filtered through blotting paper and then with Whatman no 1, followed by sterilization to get rid of the biological disturbances such as larger colloids, suspended particles, etc. This sterile lake water was further used for the toxicity studies as a freshwater matrix.

Experimental setup Bacterial cells with an initial cell count of 215×10^7 were interacted with three types of Au NPs (CIT_{30}, CIT_{40}, and CIT_{30}–PVP capped) at various concentrations of 0.25, 0.5, and 1 mg/L in sterile filtered lake water at room temperature under visible light condition. After the period of exposure (2, 4, and 6 h), cell viability was assessed using the standard plate count assay. The percentage reduction in the cell viability of the treated samples was calculated with respect to the control.

Toxicity assessment of Au NPs on algae

Test organism For algal toxicity experiments, the freshwater green alga *Chlorella* sp., a single-celled, green, and spherical-shaped microalga isolated from VIT lake, was used as the test organism (as detailed in our previous report, Iswarya et al. 2015). BG-11 broth, a specific growth medium, was used for growth and maintenance of the culture. A day/light rhythm of 16 h/8 h was maintained for the growth of algal cultures, and illumination was provided by white fluorescent lights (TL-D Super 80 linear fluorescent tubes, Phillips, India) with an intensity of 3000 lx. All the toxicity studies were carried out in a freshwater matrix, i.e., sterile lake water as per OECD guidelines (OECD, 2011).

Experimental setup At the exponential phase, algal cells were harvested from the medium by centrifugation (7000×*g*, 10 min, 4 °C) and washed with sterile lake water. Then, the algal cells with an initial cell count of about 5×10^5 cells were prepared in sterile lake water and treated with Au NPs (CIT_{30}, CIT_{40}, and CIT_{30}–PVP capped) at various concentrations of 0.25, 0.5, and 1 mg/L under visible light condition for 72 h.

Cell viability assessment After the interaction period of 72 h, the number of cells in the treated and control samples was counted using a hemocytometer under a phase contrast microscope (Zeiss Axiostar Microscope, USA). The percentage decrease in cell viability of the treated cells was calculated with respect to the control.

Toxicity assessment of the capping solution used for Au NP synthesis

Toxicity of the capping solutions used in the Au NP synthesis was analyzed to check the toxic effect of capping materials alone. Both the bacterial and algal cells were interacted with different capping agents such as citrate and PVP, similarly as done for Au NPs. The cell viability assay was performed for the capping agents, viz. 136 mM citrate (CIT_{30} Au NP), 30.4 mM citrate (CIT_{40} Au NP), and 1.25 mM PVP (CIT_{30}–PVP-capped Au NP), after interacting for 6 and 72 h for bacteria and algae, respectively. The percentage reduction in the cell viability was evaluated with respect to the control.

Biochemical assays

ROS assessment The fluorescence probe, DCFH-DA, was used to quantify the generation of reactive oxygen species (ROS). Intracellular ROS generation was measured in both control and Au NP (1 mg/L)-treated cells after the interaction period (6 h for bacteria and 72 h for algae), according to the method of Wang and Joseph (1999) with minor modifications. Five milliliters of cell suspension was incubated with DCFH-DA with a final concentration of 100 μM at 37 °C for 30 min. The fluorescence intensity of the DCFH-DA dye was measured using fluorescence spectroscopy (Cary Eclipse Fluorescence Spectroscopy; Model No: G9800A) with excitation and emission wavelengths of 485 and 530 nm, respectively.

Lactate dehydrogenase assay The extracellular lactate dehydrogenase (LDH) release was measured as an indicator of membrane permeability and cytotoxicity as per the method

reported by Dalai et al. (2012). Bacterial and algal cells were treated with 1 mg/L of Au NPs (CIT_{30}, CIT_{40}, and CIT_{30}–PVP capped) for about 6 and 72 h, respectively. After exposure, the cell suspension was centrifuged (7000×*g*, 10 min) and the LDH released in the supernatant was measured by following standard protocol. The reaction mixture contained 100 μL of the supernatant, 100 μL of 30 mM sodium pyruvate, and 100 μL of 6.6 mM NADH. LDH activity was determined as the rate of decrease in absorbance at 340 nm (UV-vis spectroscopy, Model U2910, Hitachi, Japan).

Toxicity of Au NPs towards higher organisms

Toxicity assessment of Au NPs on human cell line

Cancer cell maintenance The SiHa cell line used in this study was a kind gift from Dr. Chinmay Panda, Chittaranjan National Cancer Institute, Kolkata, India. It was an HPV16 containing cervical cancer cell line first isolated from a Japanese patient. The cells were maintained in Eagle's MEM containing sodium pyruvate, glutamine, and non-essential amino acids supplemented with 10 % FBS (Gibco) and 1× antibiotic-antimycotic solution (HiMedia) in a humidified incubator at 37 °C with 5 % CO_2.

Cytotoxicity assay Cytotoxicity of the gold nanoparticles in SiHa cells was assessed by standard MTT reduction assay (Mossman 1983). MTT is a yellow water-soluble tetrazolium dye that is reduced to purple-colored water-insoluble formazan crystals by mitochondrial dehydrogenases of viable cells. 10^3 cells were seeded in a 96-well plate and incubated overnight. Cells were then treated with Au NPs in a concentration range of 0.1 to 0.5 mg/L with regular increments of 0.1 mg/L for 24 h. Then, 100 μL of MTT (5 mg MTT/mL PBS) was added to each well, mixed, and incubated in a CO_2 incubator for another 3 h. Media were removed from the wells, and the formazan crystals were dissolved with 100 μL of DMSO (Merck). Absorbance was recorded in a microplate reader (BioRad) at 595 nm. From the absorbance data, survival percentages in treated and control sets were calculated.

DNA fragmentation DNA laddering is a hallmark of apoptotic cell death. For DNA fragmentation assay, DNA was isolated according to the method of Herrmann et al. (1994) with modification. SiHa cells were seeded in 60-mm petri dishes and incubated overnight. The cells were interacted with 1 mg/L of Au NPs (CIT_{30}, CIT_{40}, and CIT_{30}–PVP capped) for 24 h. After the interaction, the cells were harvested, washed with phosphate-buffered saline, and pelleted by centrifugation. An equal amount of 2× lysis buffer (200 mM NaCl, 20 mM Tris, 50 mM EDTA, 1 % SDS, and 2 % NP-40) was added to the pellet, mixed well, and incubated on ice for 30 min. This was followed by extraction with phenol-chloroform-isoamyl alcohol (25:24:1). Nucleic acids were collected in the aqueous phase and precipitated with isopropanol and sodium acetate. The pellet was dissolved in TE buffer and incubated with RNase A. Finally, DNA was precipitated with isopropanol and sodium acetate. Collected pellets were washed in 70 % ethanol and air-dried. DNA was dissolved in TE buffer and separated by electrophoresis on 1.5 % agarose gels.

Toxicity assessment of Au NPs on mice

Animals Healthy male Swiss albino mice (4–6 weeks old) weighing 25–30 g were purchased and acclimatized for a week in the institutional animal house. The animals belonging to the same litter (for each of the three nanoparticles and capping agents) were randomly housed in cages (seven animals per cage for each group of concentrations), maintained under standard laboratory conditions (temperature of 22±2 °C; humidity of 50–70 %, and 14 h:10 h light and dark cycle). They were kept in cages with autoclaved paddy husk for bedding and raised on standard rodent pellets (consisting of crude protein and fiber) and drinking water ad libitum throughout the study. The ethical clearance for the use of animals in the study was obtained from the institutional animal ethics committee of Calcutta University.

Treatment schedule The mice were divided into seven groups, randomly consisting of seven animals each. They were gavaged for seven consecutive days with solutions of CIT_{30}, CIT_{40}, and CIT_{30}–PVP capped Au NPs at doses of 0.01, 0.05, and 0.1 mg/kg body weight and capping agents (citrate 30.4 and 136 mM and PVP 1.25 mM) at 0.1 mL/10 g body weight (b.w.). The stock solutions Au NPs were diluted with Milli-Q water to get the following group of doses:

Group I	Mice was administered with Milli-Q water as vehicle control.
Group II	Mice were administered with Au NP solution (0.01 mg/kg b.w.).
Group III	Mice were administered with Au NP solution (0.05 mg/kg b.w.).
Group IV	Mice were administered with Au NP solution (0.1 mg/kg b.w.).
Groups V–VII	Mice were administered with solutions of capping agent (30.4 or 136 mM citrate or 1.25 mM PVP).

The animals were sacrificed by cervical dislocation on the 8th day, and the target organ, liver, was processed to evaluate oxidative stress and DNA damage.

Evaluation of DNA damage in liver cells by single-cell gel electrophoresis (comet assay) The alkaline comet assay was assessed following the method described in Tice et al. (2000) with minor alterations (Manivannan et al. 2013). Briefly, the liver tissue was minced in 0.075 M NaCl solution containing 0.024 M Na_2EDTA (pH 7.5). The cell suspension was interacted with 1 % low-melting-point agarose. Then, it was layered on the slide base that was coated with 1 % normal-melting-point agarose. The slides thus prepared were placed in the chilled lysing solution (2.5 M NaCl, 100 mM Na_2EDTA, 10 mM Trizma, 10 % DMSO, and 1 % Triton X-100, pH 10.0) for 1 h at 4 °C. Then, the slides were treated with chilled alkaline solution (300 mM NaOH and 1 mM Na_2EDTA, pH>13) for 20 min to DNA unwinding. After that, electrophoresis was performed at 0.7 V/cm and 300 mA using a freshly prepared electrophoresis buffer (1 mM EDTA disodium salt and 300 mM NaOH) at 4 °C for 25 min. After electrophoresis, the slides were neutralized with Tris buffer (400 mM, pH 7.4). The slides were stained with ethidium bromide (EtBr, 20 μg/mL) and stored at 4 °C in a humidified slide box until scoring. The slides were scored at a final magnification of ×400 using an image analysis system (Komet 5.5, Kinetic Imaging, Andor Technology, Nottingham, UK) attached to a fluorescence microscope (Leica, Germany), equipped with an attached CCD camera. Images from 150 random cells (per animal) were analyzed. The comet parameters used to measure DNA damage in the cells were tail DNA (%).

Evaluation of oxidative stress in liver Oxidative stress was indirectly measured by evaluating the amount of lipid peroxidation (LPO), reduced glutathione (GSH), glutathione *S*-transferase (GST), and catalase (CAT) in the metabolically active liver cells. The respective absorbances were read with a UV 2300 II Spectrophotometer (Techcomp Ltd., Hong Kong).

Lipid peroxidation: The lipid peroxidation level in the liver homogenates was measured using the levels of malonaldehyde (MDA), which is the end point of lipid peroxidation (Buege and Aust 1978).

GSH: The GSH level was estimated by the method of Sedlak and Lindsay (1968).

GST: The activity of GST was measured according to the method of Habig et al. (1974).

CAT: Catalase activity was monitored as per the procedure given by Abei (1984).

Protein estimation: Protein quantification in liver tissue homogenate was carried out by the method of Bradford (1976) with bovine serum albumin as standard.

More details of the above methods can be found in the Supplementary Information.

Statistical analysis

All the cytotoxicity and biochemical assays were repeated at least three times, and the data are presented as mean± standard error (SE). For the bacterial and algal cell viability assessments and also for the stability studies, the statistical analysis was performed using GraphPad Prism, Version 5.0, using two-way ANOVA ($p<0.01$). One-way ANOVA (Tukey multiple comparison test) was followed for the other assays ($p<0.05$). The data for the in vivo assays were analyzed using the Statistical Programme Sigma Stat 3.0 (SPSS Inc., Chicago, IL, USA).

Results

Characterization of Au NPs

Transmission electron micrographs of citrate- (CIT_{30} and CIT_{40}) and PVP-capped (CIT_{30}–PVP capped) Au NPs revealed that all the three types of NPs had a spherical shape (Fig. 1). The sizes were observed to be 24, 40, and 17 nm for CIT_{30}, CIT_{40}, and CIT_{30}–PVP capped Au NPs, respectively. The hydrodynamic sizes of the Au NPs (CIT_{30}, CIT_{40}, and CIT_{30}–PVP capped) were analyzed using dynamic light scattering and represented by the effective diameter. The effective diameters of the citrate-capped Au NPs (CIT_{30} and CIT_{40}) in Milli-Q water were found to be 29.01±2.42 and 43.11±0.48 nm, respectively. PVP-capped Au NPs (CIT_{30}–PVP capped) showed an effective diameter of about 65.23±3.64 nm.

The hydrodynamic sizes of the Au NPs in sterile filtered lake water and cell culture media were studied at different time intervals (0, 6, 12, and 24 h) (Fig. 2a, b). Significant ($p<0.01$) change in the effective diameter of Au NPs was observed in the sterile lake water for CIT_{30} and CIT_{40} Au NPs. The effective diameter of CIT_{30} Au NPs increased from 170.63± 5.71 nm at 0 h to 2017.26±23.48 nm after 24 h. Likewise, CIT_{40} Au NPs aggregated from 53.54±2.05 nm at 0 h to 997.39±6.39 nm after 24 h at a slower rate than CIT_{30} Au NPs. Among the citrate-capped Au NPs, CIT_{30} Au NPs aggregated more rapidly than CIT_{40} Au NPs in sterile filtered lake water. In contrast, CIT_{30}–PVP capped Au NPs were found to be highly stable in the sterile lake water, till 24 h (97.35±0.40 nm). It was also observed that CIT_{30}–PVP capped Au NPs were more stable than CIT_{30} Au NPs. The effective diameter of Au NPs in the cell culture media remained unchanged for all the three Au NPs (CIT_{30}, CIT_{40}, and CIT_{30}–PVP capped), during the experimental period of 24 h. In comparison with CIT_{30} and CIT_{40} Au NPs, the effective diameter of CIT_{40} Au NPs in the cell culture media was found to be smaller than the size of CIT_{30} Au NPs. This effect could be due to the higher reactivity of lower sized

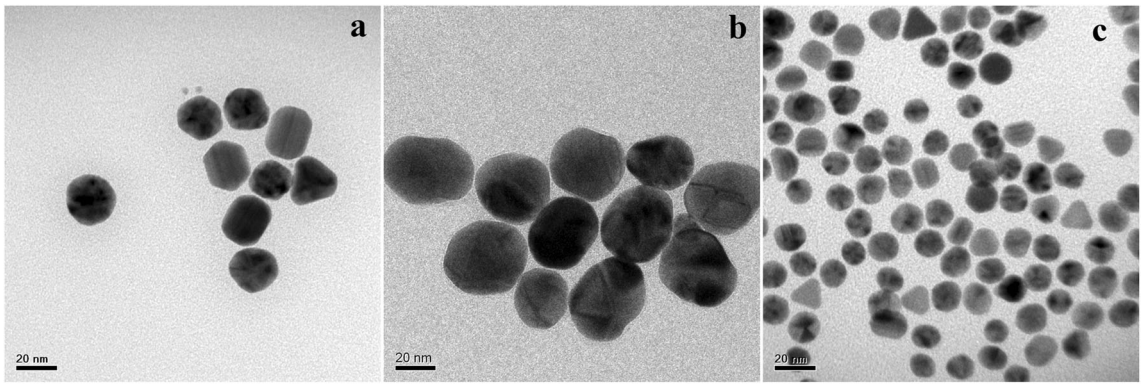

Fig. 1 Transmission electron microscopy (TEM). TEM micrograph of Au NPs: **a** CIT_{30} Au NPs, **b** CIT_{40} Au NPs, and **c** CIT_{30}–PVP capped Au NPs

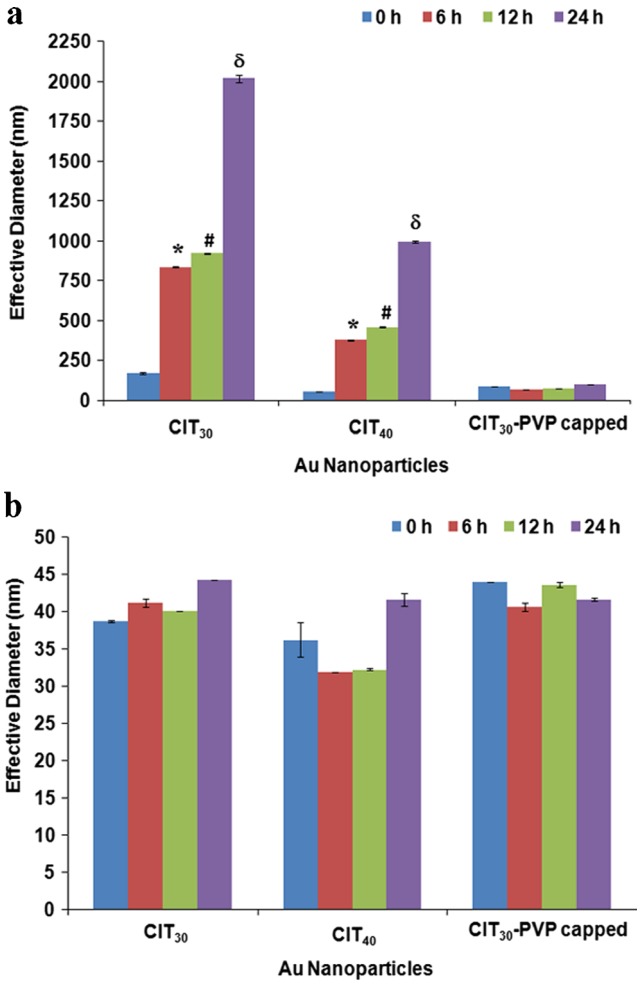

Fig. 2 Stability study of Au NPs in the different experimental matrix used in the study. Aggregation profile of different Au NPs (CIT_{30}, CIT_{40}, and CIT_{30}–PVP capped Au NPs) in the **a** sterile and filtered lake water and **b** cell culture media (Eagle's MEM). Asterisks (*) indicate that the size of the NPs at 6 h was statistically significant with respect to particle size at 0 h ($p<0.01$). The symbol # indicates that the size of the NPs at 12 h was statistically significant with respect to particle size at 6 h ($p<0.01$). The symbol δ indicates that the size of the NPs at 24 h was statistically significant with respect to particle size at 12 h ($p<0.01$)

nanoparticles to interact more readily with the components present in the cell culture media.

Toxicity of Au NPs towards lower organisms

Toxicity assessment of Au NPs on freshwater bacteria

The toxic effect of the three types of Au NPs (CIT_{30}, CIT_{40}, and CIT_{30}–PVP capped) and capping agents was analyzed on the freshwater bacterial isolate, *B. aquimaris*. Particle size-, exposure period-, and concentration-dependent decrease in the cell viability were observed for the citrate-capped Au NPs (CIT_{30} and CIT_{40}) (Fig. 3a). The viability of *B. aquimaris* cells decreased significantly ($p<0.01$) with increasing period of exposure. With a decrease in particle size, the toxicity of citrate-capped Au NPs increased ($CIT_{30}>CIT_{40}$). The cell viability decreased significantly with respect to the exposure period and concentration of PVP-capped Au NPs (CIT_{30}–PVP capped). Between CIT_{30} and CIT_{30}–PVP capped Au NPs, CIT_{30} Au NPs showed higher toxicity than CIT_{30}–PVP capped Au NPs. It clearly shows that surface capping (PVP) reduced the cytotoxicity of gold nanoparticles.

Capping agents used in the synthesis such as citrate (136 and 30.4 mM) and PVP (1.25 mM) were considered as a vehicle control, and their toxic effect has been evaluated similarly. Among the three capping controls, 1.25 mM PVP solution caused a significant ($p<0.05$) reduction in the viability of cells than citrate solution (Fig. 3b).

The generation of reactive oxygen species in bacteria after an interaction (6 h) with 1 mg/L of Au NPs (CIT_{30}, CIT_{40}, and CIT_{30}–PVP capped) was evaluated by dichlorofluorescein diacetate (DCFH-DA) (Fig. 4a). The increase in fluorescence intensity was statistically significant ($p\leq0.05$) and related to the particle size of citrate-capped Au NPs. CIT_{30}–PVP capped Au NPs showed less ROS production than CIT_{30} Au NPs.

The cell membrane integrity was compromised by the Au NPs as revealed in the LDH assay (Fig. 4b). The release in the LDH content of 1 mg/L of Au NPs in bacteria increased

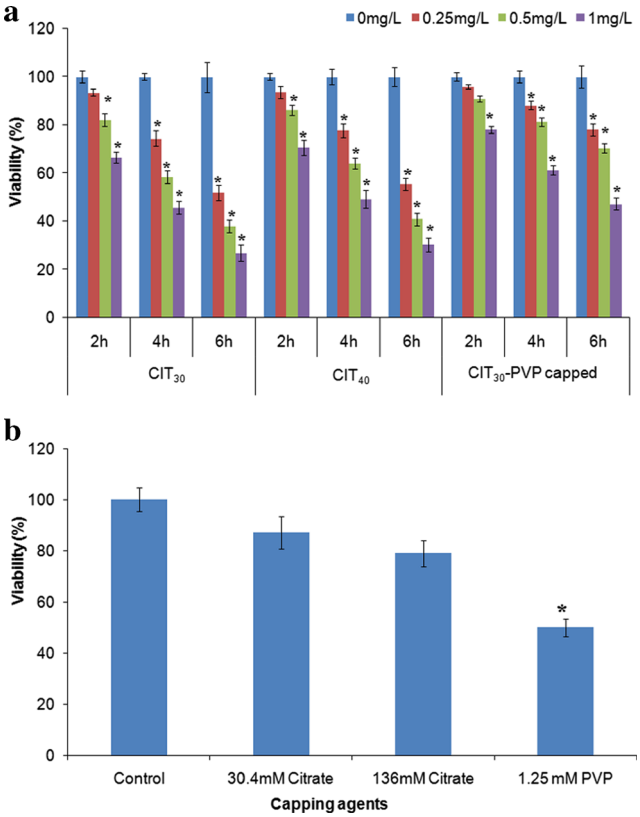

Fig. 3 Cytotoxicity assessment of Au NPs on *Bacillus aquimaris*. Cell viability of *Bacillus aquimaris* on exposure to **a** different concentrations of different Au nanoparticles at various exposure periods (2, 4, and 6 h), * significant with respect to control, $p<0.01$, and **b** capping agents after 6 h interaction, * significant with respect to control, $p<0.05$

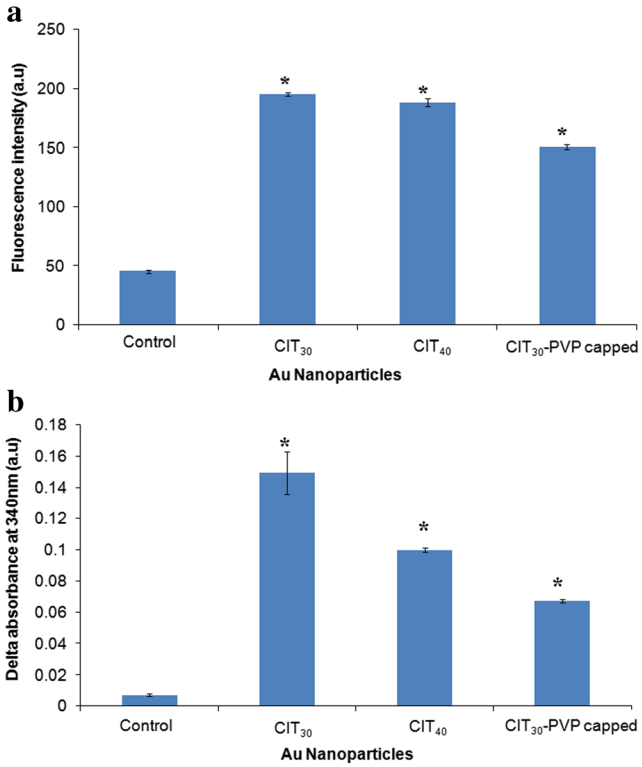

Fig. 4 Biochemical assays revealing the toxic mechanism by the Au NPs on *Bacillus aquimaris*. **a** Oxidative stress (ROS) assessment of bacterial cells after 6 h interaction with various Au NPs (1 mg/L), **b** LDH release after 6 h interaction of *Bacillus aquimaris* with various Au NPs (1 mg/L). * Significant with respect to control, $p<0.05$

significantly ($p<0.05$) than that of the control. ROS production and cell membrane damages were higher in CIT_{30} Au NPs than those in other Au NPs.

Toxicity assessment of Au NPs on freshwater green algae

The effect of Au NPs (CIT_{30}, CIT_{40}, and CIT_{30}–PVP capped) and capping agents was studied on the freshwater algal isolate *Chlorella* sp. On exposure to CIT_{30} and CIT_{40} Au NPs (1 mg/L), the cell viability was found to be 46.84±0.69 and 52.46±0.77 %, respectively. Toxicity was found to be particle size and concentration dependent (Fig. 5a). Similar to bacteria, the highest toxicity was observed for CIT_{30} Au NPs than other sizes. Upon exposure to CIT_{30}–PVP capped Au NPs, the cell viability was found to be about 64.56±3.29 % at the concentration of 1 mg/L. As in bacteria, CIT_{30} Au NPs showed higher toxicity than CIT_{30}–PVP capped Au NPs in *Chlorella* sp.

Cell viability in the treatment with the capping agents was 92.41±1.52, 88.78±3.66, and 72.51±2.43 % for 30.4 mM citrate, 136 mM citrate, and 1.25 mM PVP, respectively. The PVP solution (1.25 mM) induced a significant reduction in viability ($p<0.05$) than the citrate solutions (Fig. 5b).

Reactive oxygen species (ROS) generation for treated and control algal cells is represented in Fig. 6a. Significant ROS production ($p<0.05$) was observed in CIT_{30} and CIT_{40} Au NPs. Analogous to the cell viability results, the ROS production increased with the decrease in particle size. Compared to the control, ROS generation induced by CIT_{30}–PVP capped Au NPs was found to be insignificant.

The release of the cytoplasmic enzyme, LDH, in the treated and control algal cells is represented in Fig. 6b. LDH release was found to be significantly high ($p<0.05$) in CIT_{30}–PVP capped-interacted algal cells than the control. In CIT_{30} and CIT_{40} Au NP-interacted algal cells, LDH release was found to be insignificant.

Toxicity of Au NPs towards higher organisms

Assessment of toxicity of Au NPs on SiHa cell line

The cytotoxicity induced by the capping agents and Au NPs was determined by MTT assay in the SiHa cell line. The capping agents used in the present study did not induce any cytotoxicity in SiHa cells (Fig. 7a). At an exposure period of 24 h, the survival rate of the SiHa cells exposed to CIT_{30} Au NPs was significantly less than that

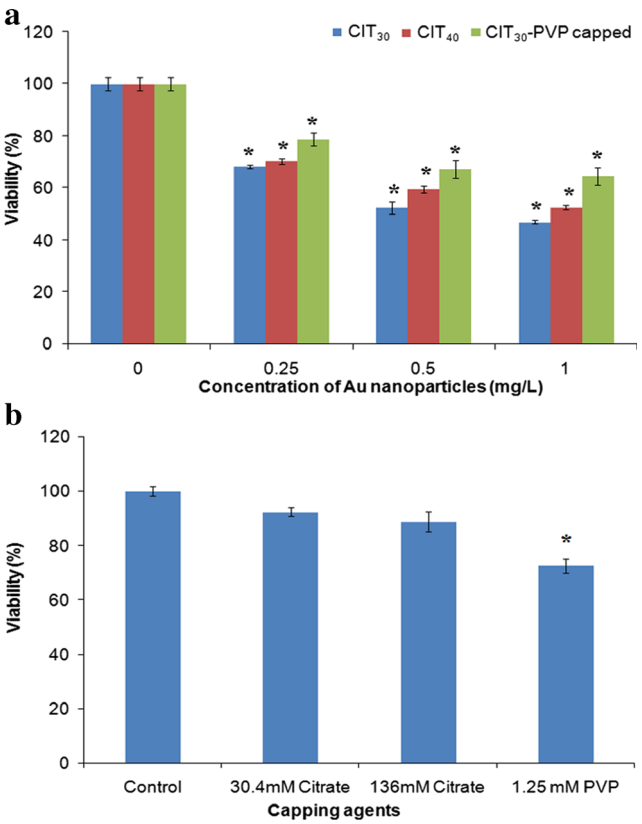

Fig. 5 Cytotoxicity evaluation of Au NPs on *Chlorella* sp. Cell viability of *Chlorella* sp. on exposure to **a** different concentrations of different Au nanoparticles, i.e., CIT_{30}, CIT_{40}, and CIT_{30}–PVP capped Au NPs after 72 h, * significant with respect to control, $p<0.01$, and **b** capping agents after 72 h interaction, * significant with respect to control, $p<0.05$

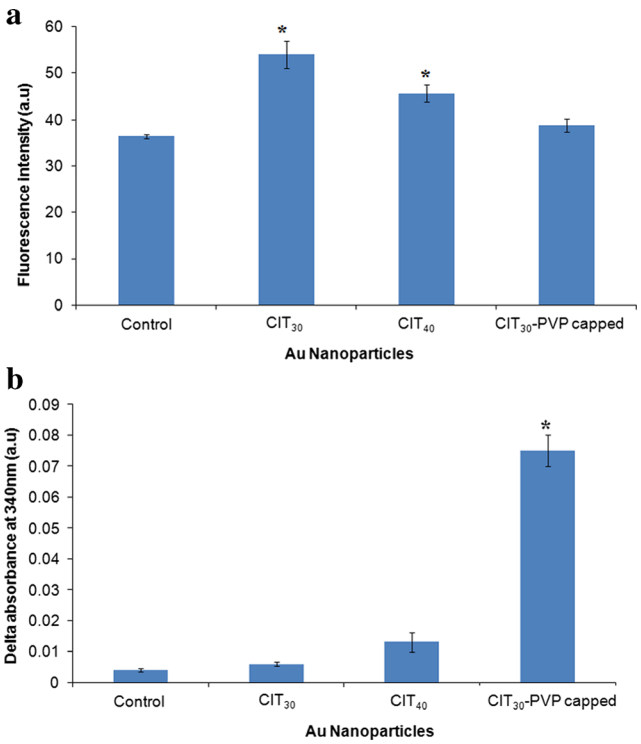

Fig. 6 Biochemical assays revealing the toxic mechanism by the Au NPs on *Chlorella* sp. **a** Oxidative stress assessment after 72 h interaction of algal cells with various Au NPs (1 mg/L). **b** LDH release after 72 h interaction of algal cells with various Au NPs (1 mg/L). * Significant with respect to control, $p<0.05$

of the control at the concentration 0.5 mg/L (Fig. 7b). With increasing concentration (0.1 to 0.5 mg/L) and period of exposure (48 and 72 h), the survival rate of cells decreased gradually and was statistically significant in CIT_{30}, CIT_{40}, and CIT_{30}–PVP capped Au NP sets (Fig. 7c, d). In general, the survival rate decreased with increasing concentration of the Au NPs and the period of exposure used. A higher impairment of cell viability was noted for CIT_{30} Au NPs. The suppressive effect of Au NPs was indirectly associated with their sizes in SiHa cells.

Distinct genomic DNA bands without any laddering were observed (Fig. 8). The absence of DNA laddering supports that there was no apoptotic cell death of the SiHa cells.

Toxicity assessment of Au NPs on mice model

DNA strand breaks in liver cells of mice after oral treatment with Au NPs and the different capping agents used for the synthesis are presented in panels a and b of Fig. 9, respectively. Of the two sizes of citrate-capped Au NPs, the percent tail DNA was significantly higher in CIT_{30} Au NPs than that in CIT_{40} Au NPs. Functionalizing CIT_{30} Au NPs with PVP also caused an increase in DNA strand breaks leading to greater DNA migration out of the nucleus into the tail of the comet. In general, exposure to various concentrations of Au NPs (0.01, 0.05, and 0.10 mg/kg body weight) enhanced DNA fragmentation. The induction of DNA damage was directly dependent on the size of the Au NPs and their concentration in solution. With respect to the vehicle control, citrate capping (136 mM) induced significantly more DNA strand breaks.

Effects of exposure to different types of Au NP caused an alteration of the oxidative stress-related end points in mice hepatocytes. The results of lipid peroxidation are represented in Fig. 10a, b. As compared to the control, MDA level was markedly increased by citrate-capped Au NPs (CIT_{30} and CIT_{40}). The lipid peroxide level was significantly increased in the treatment with citrate-capped Au NPs, CIT_{30}, at the concentration of 0.05 mg/kg b.w. and with CIT_{40} at concentrations of 0.01 and 0.05 mg/kg b.w. Citrate as a capping agent has caused a statistically significant rise in the level of MDA content in the tissue. Administration of PVP (1.25 mM) and functionalizing CIT_{30} Au NPs with PVP did not generate much reactive oxygen species. Hence, there was no significant rise in cellular MDA content with respect to the control.

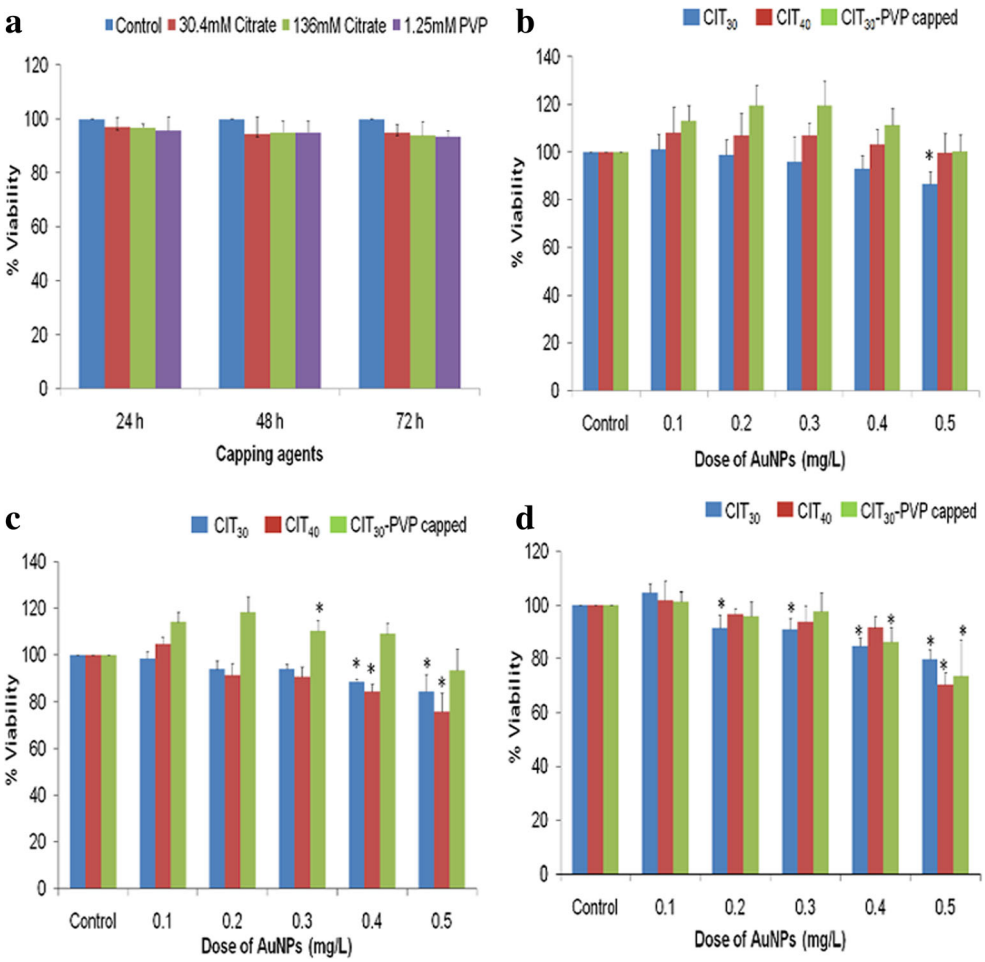

Fig. 7 Cytotoxicity evaluations of Au NPs on SiHa cell line. **a** Cell viability assessment with different capping agents, **b** SiHa cells exposed to Au NPs for 24 h, **c** SiHa cells exposed to Au NPs for 48 h, and **d** SiHa cells exposed to Au NPs for 72 h. * Significant with respect to control, $p \leq 0.05$

A decrease in GSH corresponds to increased oxidative stress due to ROS generation. In the present study, GSH levels decreased in cells exposed to the lowest concentration (0.01 mg/kg b.w.) of CIT_{40} Au NPs and at all concentrations for CIT_{30}–PVP capped Au NPs (Fig. 11a). The consumption of glutathione for scavenging of ROS did not follow a dose-dependent trend for the various concentrations of CIT_{30} Au NPs. Citrate (30.4 mM) and PVP (1.25 mM) did not induce a positive response (Fig. 11b).

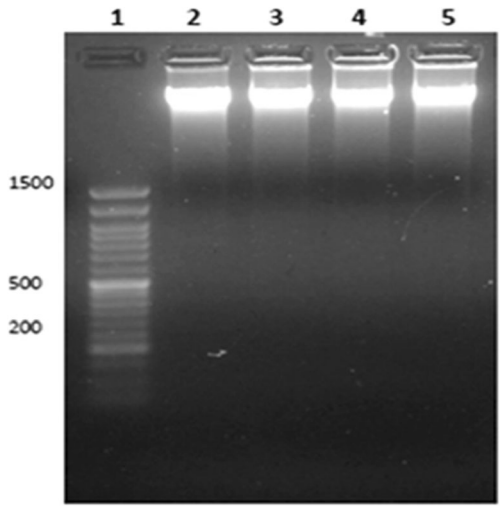

Fig. 8 DNA fragmentation assay. Agarose gel showing the intact genomic DNA bands. *Lane 1*: 100-bp marker, *lane 2*: control, *lane 3*: CIT_{30} Au NPs, *lane 4*: CIT_{40} Au NPs, *lane 5*: CIT_{30}–PVP capped Au NPs

The GST activity following exposure to different sizes and concentrations of gold nanoparticles (CIT_{30} and CIT_{40}) did not show a dose-dependent change except for CIT_{30}–PVP capped, where the level of GST has decreased significantly at all the concentrations with respect to the control (Fig. 12a). PVP (1.25 mM) as capping agent has caused a statistically significant decrease in GST activity (Fig. 12b). The cellular responses (in terms of GSH) to the various concentrations of citrate capping were more or less similar to that of the control ones.

The catalase activities of Au NPs (CIT_{30}, CIT_{40}, and CIT_{30}–PVP capped) are represented in Fig. 13a. There was a significant rise in catalase activity in cells exposed to Au NPs (CIT_{30}–PVP capped) at the concentration 0.05 mg/kg b.w. Catalase activity remained unaffected in CIT_{30} Au NPs and decreased significantly (when compared to the control) in liver cells exposed to CIT_{40} Au NPs (at concentrations of 0.05

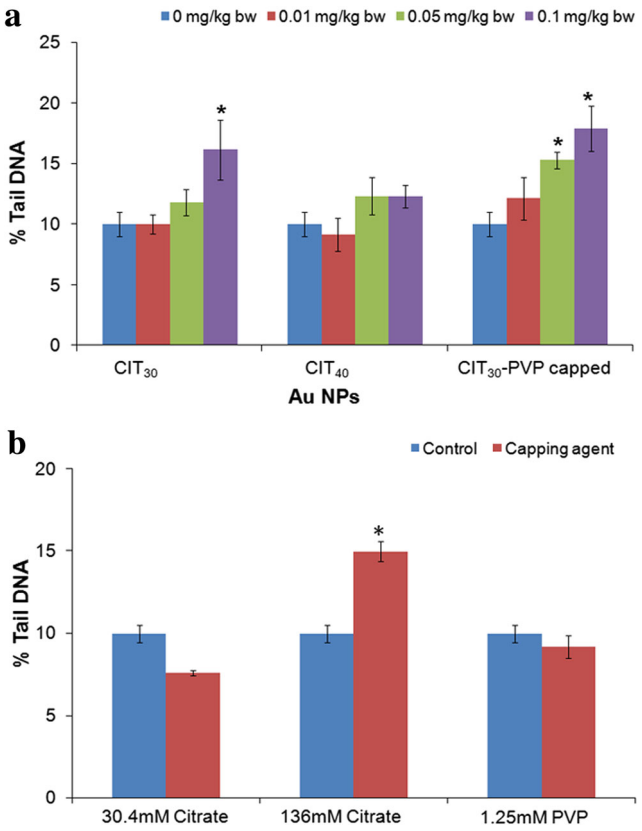

Fig. 9 DNA strand break assay on mice model. Assessment of DNA strand breaks in liver cells of mice exposed to treatment with **a** different sizes and concentrations of gold nanoparticles (Au NPs). **b** Capping agents. * Significant with respect to control, $p \leq 0.05$

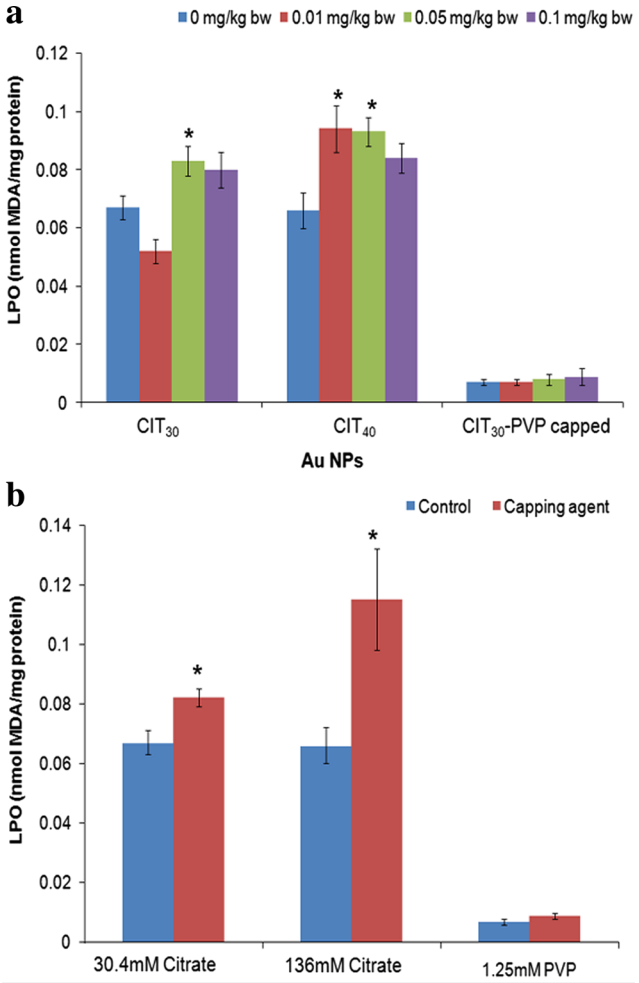

Fig. 10 Lipid peroxidation assay. Assessment of lipid peroxidation in liver cells of mice exposed to treatment with **a** different sizes and concentrations of gold nanoparticles (Au NPs). **b** Capping agents. * Significant at $p \leq 0.05$ with respect to control

and 0.1 mg/kg b.w.). The catalase activity of the capping agent PVP was significantly high (Fig. 13b).

Discussion

There are a significant number of studies on the genotoxicity and cytotoxicity of Au NPs on mammalian cell lines (Alkilany and Murphy 2010; Chueh et al. 2014; Coradeghini et al. 2013). The majority of nanotoxicity research has focussed on cell culture. We evaluated the overall toxicological impact of Au NPs in organisms of diverse trophic levels. They included bacteria (*B. aquimaris*), an alga (*Chlorella* sp.), a cervical cancer cell line (SiHa), and Swiss albino mice. Since an appropriate coating of nanoparticles ensures stability as well as partially prevents their harmful effects, we have coated the Au NPs with citrate and PVP for the possibility of producing safer Au NPs. Before studying the toxic potential of Au NPs, we characterized their size by dynamic light scattering as well as TEM.

Physicochemical characterization of Au NPs showed a typical TEM image of round-shaped Au NPs. The size of the CIT_{30}–PVP capped Au NPs was slightly reduced from the size of CIT_{30} Au NPs that might be due to the addition of PVP solution. Pillai and Kamat (2004) cited that the covalent linkage or surface capping of nanoparticles with an organic molecule usually yields smaller sized NPs. The size of the citrate-capped Au NPs (CIT_{30} and CIT_{40} Au NPs) obtained from the TEM was found to be in agreement with the DLS results, while in CIT_{30}–PVP capped Au NPs, a large variation between the DLS and TEM was noted. Nur (2013) illustrated that the difference between DLS and TEM size is always higher for the PVP-stabilized samples than the citrate-stabilized samples. This size difference was due to the PVP, a long-chain polymer whose size is larger than that of citrate, a much smaller molecule (Tejamaya et al. 2012).

DLS is a highly sensitive, analytical tool recommended for monitoring nanoparticle aggregation in solution (Diegoli et al. 2008; Jans et al. 2009; Powers et al. 2006). In the present study, DLS has been used as the primary size determination tool to analyze the aggregation rate of Au NPs in the respective experimental matrix such as sterile lake water and cell culture media. The effective diameter of CIT_{30} Au NPs in

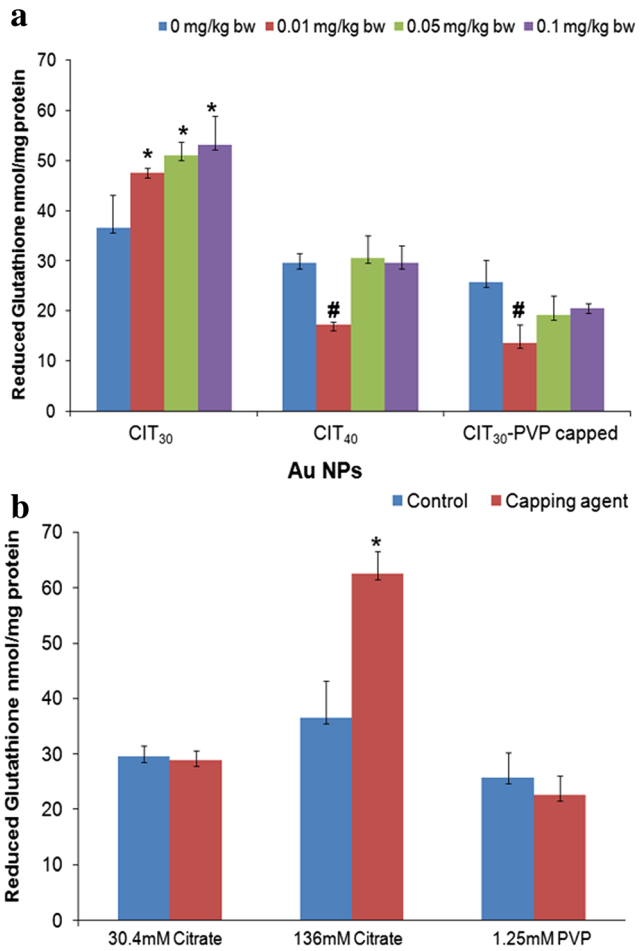

Fig. 11 GSH activity. Assessment of GSH activity in liver cells of mice exposed to treatment with **a** different sizes and concentrations of gold nanoparticles (Au NPs). * Significantly higher with respect to control at $p \leq 0.05$; # significantly lower with respect to control at $p \leq 0.05$. **b** Capping agents. * Significant with respect to control at $p \leq 0.05$

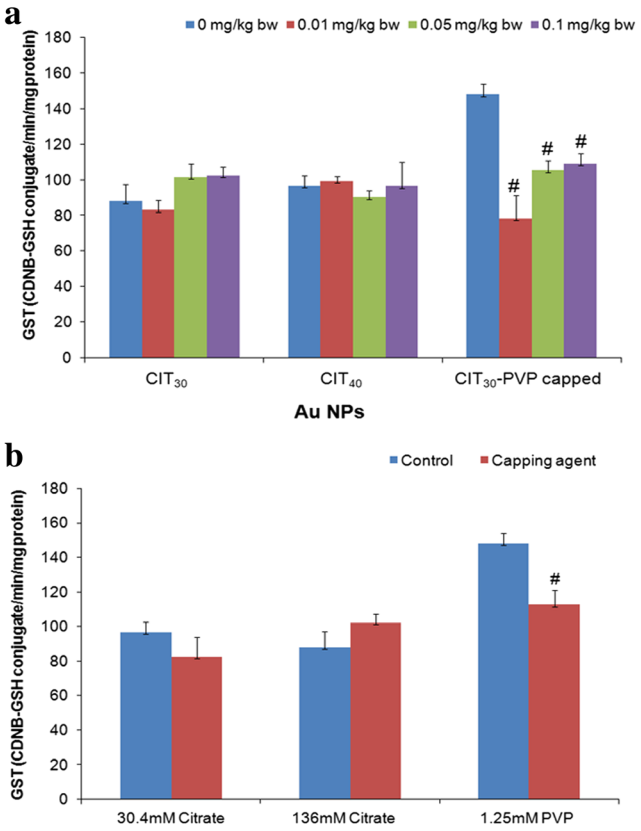

Fig. 12 GST activity. Assessment of GST activity in liver cells of mice exposed to treatment with **a** different sizes and concentrations of gold nanoparticles (Au NPs). **b** Capping agents. # Significantly lower with respect to control at $p \leq 0.05$

sterile lake water was increased at 0 h to more than 100 nm. This effect was not found in CIT_{40} and CIT_{30}–PVP capped Au NPs, which could be due to the higher reactivity of lower sized nanoparticles (CIT_{30}). According to Zeng et al. (2012), the surface energy of Au NPs increases, as the diameter decreases; as a result, smaller Au NPs interact more strongly with the compounds present in the solution and leads to size-dependent aggregation of Au NPs. In sterile lake water, CIT_{30} Au NPs agglomerated rapidly than CIT_{40} Au NPs. The DLS results depicted that PVP-capped Au NPs (CIT_{30}–PVP capped) were more stable than the citrate-capped Au NPs (CIT_{30} and CIT_{40}). Similar results were observed by Nur (2013) in environmentally relevant ionic strength solutions and bacterial growth media. The effect of natural organic matter (NOM, Suwannee River humic acid) on the aggregation rate of Au NPs stabilized with various capping agents was demonstrated by Stankus et al. (2011). They reported that due to the variations in ionic strength and pH, the rate of aggregation was high for citrate-capped Au NPs. In general, the citrate-capped Au NPs rely on the electrostatic interactions of citrate and are weakly bound to Au NPs (Tolaymat et al. 2010). But, polyvinyl pyrrolidone (PVP) relies on steric stabilization and is strongly bound to the core of NPs (Römer et al. 2011; Cumberland and Lead 2009). Thus, the charge-stabilized nanoparticles (citrate capped) were more unstable in the lake water than the sterically stabilized nanoparticles (PVP capped).

In contrast to the sterile lake water matrix, the hydrodynamic size of the Au NPs in the culture media was found to be unchanged for all the three types of Au NPs, during the experimental period of 24 h. The biological components of media such as proteins, etc. might have helped in the stabilization of Au NPs and thereby prevented the aggregation of nanoparticles due to the formation of protein corona or biomolecular coating on NPs (Cedervall et al. 2007).

In both bacteria and algae, the toxic effect of citrate-capped Au NPs was dependent on the particle size and concentration. These results are in agreement with the size-dependent toxicity reported by Coradeghini et al. (2013) and Pan et al. (2007) in several cell lines. Previous information on the toxicity of Au NPs in various organisms suggested that surface chemistry and charged surface functional groups of the Au NPs play a crucial role in determining their cellular toxic effects (Bozich

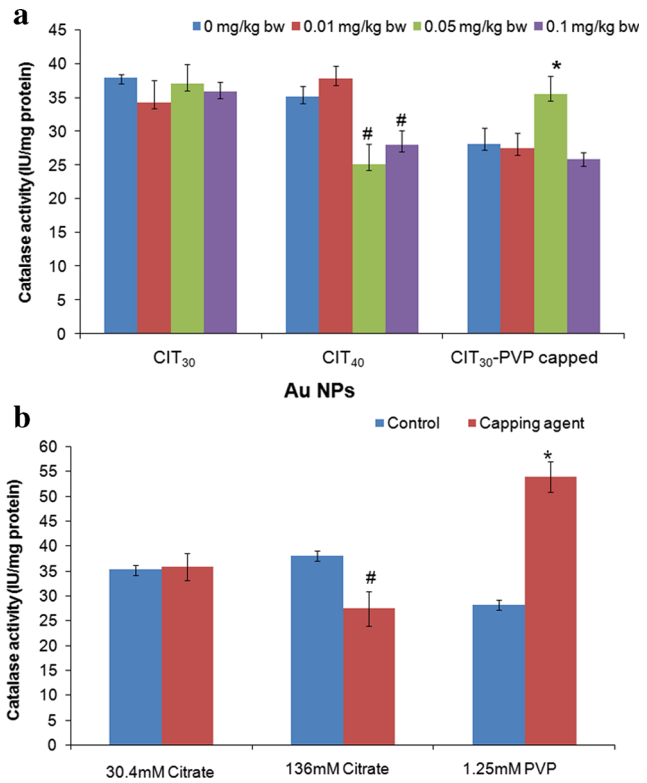

Fig. 13 Catalase activity. Assessment of catalase activity in liver cells of mice exposed to treatment with **a** different sizes and concentrations of gold nanoparticles (Au NPs). **b** Capping agents. * Significantly higher with respect to control at $p \leq 0.05$; # significantly lower with respect to control at $p \leq 0.05$

et al. 2014; Kim et al. 2013). In our study, PVP-capped gold nanoparticles showed lesser toxicity than citrate-capped nanoparticles in the case of both bacteria and algae. Sathishkumar et al. (2014) mentioned that the protective coating of nanoparticles reduced the cytotoxicity and helped in the stabilization of nanoparticles. These findings suggest that the size and surface capping of the nanoparticles may play an important role in the cytotoxicity of Au NPs.

Mechanisms of toxicity implicated by the Au NPs in bacteria and algae were confirmed by the ROS and LDH assay. In bacteria, ROS generation and LDH release were dependent on the size and surface capping of Au NPs. Higher ROS generation and cell membrane damage were observed in CIT_{30} Au NPs compared to CIT_{40} and CIT_{30}–PVP capped Au NPs. In contrast, a different mechanism might have been followed for Au NP toxicity on the algal cells. For algal cells, ROS generation seemed to be the major contributor in the toxicity of citrate-capped Au NPs (CIT_{30} and CIT_{40}). In the case of CIT_{30}–PVP capped Au NPs, enhanced membrane damage could be significantly imparting its toxicity.

In the bacteria model, the LDH release and ROS generation were well correlated for both citrate- and PVP-capped Au NPs. But in algae, enhanced LDH release by the CIT_{30}–PVP capped Au NPs was found to be inconsistent with the decreased ROS generation. There can be numerous possible reasons for this discrepancy. Wang et al. (2011) reported that the oxidation of Au^{3+} ions and decarboxylation of citrate on the surface of Au NPs induced the generation of free radicals in the presence of light. Due to the unavailability of reactive citrate ions on the surface of PVP-capped Au NPs, CIT_{30}–PVP capped Au NPs induced less ROS generation than the citrate-capped Au NPs (CIT_{30} and CIT_{40}) in both bacteria and algae. The cell wall of algae is primarily made up of cellulose; while in the case of bacteria, the cell wall majorly consists of peptidoglycan (Cooper 2000; Remade 1990). Due to the variation in the cell wall structure, interaction between the CIT_{30}–PVP capped Au NPs and the algal cell wall may be enhanced in comparison to that in bacteria. Renault et al. (2008) observed a specific surface interaction/adsorption of amine-coated Au NPs on the cell walls of *Scenedesmus subcapitus*. The effect of capping agents alone (citrate and PVP) on ROS generation and LDH release in algae was also studied. Following the LDH release and ROS generation data for CIT_{30}–PVP capped Au NPs (Fig. 6), 1.25 mM PVP also showed enhanced membrane damage (0.49±0.26 a.u.) than citrate (0.10±0.05 and 0.09±0.03 a.u. for 136 and 30.4 mM, respectively) with respect to the control. However, PVP induced less ROS generation (27.37±5.13 a.u.) than the citrate (54.62±3.27 a.u. for 136 mM and 33.06 a.u. for 30.4 mM) in comparison to the control.

Previous in vitro studies have shown that the presence of sodium citrate residues on the particle surface resulted in a decline in cell viability of epithelial and endothelial cells (Freese et al. 2012). The cytotoxicity induced by the capping agents and Au NPs was determined by MTT assay in vitro in the SiHa cell line. This cell model was specifically selected based on prior reports regarding extensive application of Au NPs for cancer cell imaging and therapeutics in SiHa cells (Gao et al. 2012; Kumar et al. 2011; Leonard et al. 2011). The concentrations selected were based on our in vivo studies and previous studies (Kumar et al. 2011; Leonard et al. 2011). In general, the survival rate decreased with increasing concentration of the Au NPs and the period of exposure. The suppressive effect of Au NPs was indirectly associated with their sizes in SiHa cells, and distinct genomic DNA bands without any DNA laddering support that there was no apoptotic cell death of the SiHa cells. There is only a handful of previous reports with regard to apoptosis signaling and onset after cell exposure to Au NPs.

In the present study, genotoxic potentials of the Au NPs (CIT_{30}, CIT_{40}, and CIT_{30}–PVP capped) were investigated using the alkaline comet assay in vivo on mice hepatocytes. The liver was the preferred organ of study as it is the target site where Au NPs are generally deposited (Chen et al. 2013; Khan et al. 2013; Simpson et al. 2013). Selection of dose for in vivo nanotoxicity experiments is interlaced with many challenges that include stability and dispersion of the nanoparticle

used (Dhawan and Sharma 2010). There are a number of previous in vivo toxicity studies involving low dose levels of Au NPs (Lasagna-Reeves et al. 2010; Cho et al. 2009; Zhang et al. 2009). Alkaline comet assay experiments detect many types of DNA damage, i.e., strand breaks, alkali-labile sites, and incomplete excision repair sites (Kumaravel and Jha 2006). Au NPs possibly induced some or all of these types of DNA damage. The induced DNA damage was directly dependent on the size of the Au NPs and their concentration in solution. Irrespective of the capping agent, CIT_{30} and CIT_{30}–PVP capped Au NPs induced significant DNA damage. Citrate at higher concentration (136 mM) induced significant DNA damage. However, the intratracheal instillation of uncoated gold nanomaterials of 2-, 20-, and 200-nm sizes investigated for DNA damage revealed a weak size-related increase of the mean tail intensity (Schulz et al. 2012). Hwang et al. (2012) reported significant differences in toxicity of Au NPs in the livers of mice, depending on the diet given to the experimental animals (methionine- and choline-deficient diet, viz. normal chow diet). Therefore, specific effects of size and surface functionalization of nanoparticles cannot be simply distinguished, and further in-depth studies were required to obtain more clarity on this issue.

Au NPs have been shown to induce a variety of toxic effects, including generation of reactive oxygen species and oxidative stress (Li et al. 2010; Tedesco et al. 2010; Gao et al. 2011). In the current study, Au NPs exerted oxidative stress causing substantial damage to different cellular components, DNA breaks, and lipid membrane peroxidation. Further studies on Au NPs revealed that Au NPs induced the formation of reactive oxygen species (ROS) and increased the level of lipid peroxidation. The activities of glutathione peroxidase (GSH), catalase (CAT), and the content of glutathione (GST) did not follow a dose-dependent trend for the various concentrations and sizes of the Au NPs used. Several recent reports have shown ROS generation in the cells exposed to Au NPs. Li et al. (2010) showed an increased oxidative stress and lipid peroxidation in MRC-5 (human lung fibroblasts) cells exposed to Au NPs. Tedesco et al. (2010) also reported an increase in oxidative stress upon in vivo exposure of Au NPs. Gao et al. (2011) demonstrated GSH depletion induced hydrogen peroxide generation in HL7702 (human liver cell line) cells upon exposure to Au NPs.

Summary and conclusions

This study aimed to address the toxicity of gold nanoparticles relevant to their size and surface functionalization on diverse organisms. In general, the physicochemical properties of Au NPs (i.e., size and surface modifications) influenced the interaction with the different trophic levels studied in vitro (bacteria, algae, SiHa cell line) and in vivo (mice). Beyond the variability of experimental conditions related to the organisms selected, in general, as-synthesized Au NPs were significantly toxic both in vitro and in vivo. CIT_{30} Au NPs were most toxic to bacterial, algal, and SiHa cells. The addition of PVP over CIT_{30} Au NPs reduced the toxic effects across trophic levels. However, in the mice model, genotoxicity was found to be increased upon exposure to CIT_{30}–PVP capped Au NPs as compared to CIT_{30} Au NPs. The capping agent, PVP, which is a long-chain polymer was individually inert in the majority of the biological targets tested. In summary, results from this study provide a comprehensive understanding of size- and surface functionalization-dependent toxic effects of Au NPs across the trophic levels.

Acknowledgments The authors would like to thank the Advanced Facility for Microscopy and Microanalysis (AFMM), Indian Institute of Science, Bangalore, for the transmission electron microscopy facility and the Center for Research in Nanoscience and Nanotechnology (CRNN), University of Calcutta, for the instrumentation facilities.

Compliance with ethical standards For the mice model study, the ethical clearance for the use of animals in the study was obtained from the institutional animal ethics committee.

Conflict of interest The authors declare that they have no competing interests.

References

Abei H (1984) Catalase in vitro. Methods Enzymol 105:121–126

Alkilany AM, Murphy CJ (2010) Toxicity and cellular uptake of gold nanoparticles: what we have learned so far? J Nanoparticle Res 12: 2313–2333

Anker JN, Hall WP, Lyandres O, Shah NC, Zhao J, Van Duyne RP (2008) Biosensing with plasmonic nanosensors. Nat Mater 7:442–453

Aruoja V, Dubourguier H, Kasemets K, Kahru A (2009) Toxicity of NPs of CuO, ZnO and TiO_2 to microalgae *Pseudokirchneriella subcapitata*. Sci Total Environ 407(4):1461–1468

Behra R, Wagner B, Sgier L, Kistler D (2015) Colloidal stability and toxicity of gold nanoparticles and gold chloride on *Chlamydomonas reinhardtii*. Aquat Geochem 21(2-4):331–342

Bozich JS, Lohse SE, Torelli MD, Murphy CJ, Hamers RJ, Klaper RD (2014) Surface chemistry, charge and ligand type impact the toxicity of gold nanoparticles to Daphnia magna. Environ Sci Nano 1(3): 260–270

Bradford MM (1976) A rapid and sensitive method for the quantitation of microgram quantities of protein utilizing the principle of protein-dye binding. Anal Biochem 72:248–254

Buege JA, Aust SD (1978) Microsomal lipid peroxidation. Methods Enzymol 52:302–311

Cedervall T, Lynch I, Lindman S, Berggård T, Thulin E, Nilsson H, Dawson KA, Linse S (2007) Understanding the nanoparticle–protein corona using methods to quantify exchange rates and affinities of proteins for nanoparticles. Proc Natl Acad Sci U S A 104(7): 2050–2055

Chen H, Dorrigan A, Saad S, Hare DJ, Cortie MB, Valenzuela S (2013) In vivo study of spherical gold nanoparticles: Inflammatory effects

and distribution in mice. PLoS ONE 8(2):e58208. doi:10.1371/journal.pone.0058208
Cho WS, Cho M, Jeong J, Choi M, Cho HY, Han BS, Kim SH, Kim HO, Lim YT, Chung BH, Jeong J (2009) Acute toxicity and pharmacokinetics of 13 nm-sized PEG-coated gold nanoparticles. Toxicol Appl Pharmacol 236:16–24
Chuang S, Lee Y, Liang R, Roam G, Zeng Z, Tu H, Wang S, Chueh P (2013) Extensive evaluations of the cytotoxic effects of gold nanoparticles. Biochim Biophys Acta 1830:4960–4973
Chueh P, Liang R, Lee Y, Zeng Z, Chuang S (2014) Differential cytotoxic effects of gold nanoparticles in different mammalian cell lines. J Hazard Mater 264:303–312
Cooper GM. (2000) Cell walls and the extracellular matrix. In: The cell: a molecular approach. 2nd edn. Sinauer Associates, Sunderland (MA). Available from: http://www.ncbi.nlm.nih.gov/books/NBK9874/. Accessed 22 September 2015
Coradeghini R, Gioria S, García CP, Nativo P, Franchini F, Gilliland D, Ponti J, Rossi F (2013) Size-dependent toxicity and cell interaction mechanisms of gold nanoparticles on mouse fibroblasts. Toxicol Lett 217:205–216
Cumberland SA, Lead JR (2009) Particle size distribution of silver nanoparticles at environmentally relevant conditions. J Chromatogr A 1216:7
Dalai S, Pakrashi S, Suresh Kumar RS, Chandrasekaran N, Mukherjee A (2012) A comparative cytotoxicity study of TiO_2 nanoparticles under light and dark conditions at low exposure concentrations. Toxicol Res 1(2):116–130
Dhawan A, Sharma V (2010) Toxicity assessment of nanomaterials: methods and challenges. Anal Bioanal Chem 398:3996
Diegoli S, Manciulea AL, Begum S, Jones IP, Lead JR, Preece JA (2008) Interaction between manufactured gold nanoparticles and naturally occurring organic macromolecules. Sci Total Environ 402:51–61
Eustis S, El-Sayed MA (2006) Why gold nanoparticles are more precious than pretty gold: noble metal surface plasmon resonance and its enhancement of the radiative and nonradiative properties of nanocrystals of different shapes. Chem Soc Rev 35:209–217
Freese C, Uboldi C, Gibson MI, Unger TE, Weksler BB, Romero IA, Couraud PO, Kirkpatrck JC (2012) Uptake and cytotoxicity of citrate-coated gold nanospheres: comparative studies on human endothelial and epithelial cells. Part Fibre Toxicol 9:23–32
Gao W, Xu K, Ji L, Tang B (2011) Effect of gold nanoparticles on glutathione depletion induced hydrogen peroxide generation and apoptosis in HL7702 cells. Toxicol Lett 205:86–95
Gao J, Huang X, Liu H, Zan F, Ren J (2012) Colloidal stability of gold nanoparticles modified with thiol compounds: bioconjugation and application in cancer cell imaging. Langmuir 28(9):4464–4471
Habig WH, Pabst MJ, Jakoby WD (1974) Glutathione S-transferases, the first enzymatic step in mercapturic acid formation. J Biol Chem 249: 7130–7139
Herrmann M, Lorenz HM, Voll R, Grunke M, Woith W, Kalden JR (1994) A rapid and simple method for the isolation of apoptotic DNA fragments. Nucleic Acids Res 22:5506–5507
Hoecke KV, De Schamphelaere KAC, Ali Z, Zhang F, Elsaesser A, Rivera-Gil P, Parak WJ, Smagghe G, Howard CV, Janssen CR (2013) Ecotoxicity and uptake of polymer coated gold nanoparticles. Nanotoxicology 7(1):37–47
Hwang JH, Kim SJ, Kim YH, Noh JR, Gang GT, Chung BH, Song NW, Lee CH (2012) Susceptibility to gold nanoparticle-induced hepatotoxicity is enhanced in a mouse model of nonalcoholic steatohepatitis. Toxicology 294:27–35
Iswarya V, Bhuvaneshwari M, Alex SA, Iyer S, Chaudhuri G, Chandrasekaran PT, Bhalerao GM, Chakravarty S, Raichur AM, Chandrasekaran N, Mukherjee A (2015) Combined toxicity of two crystalline phases (anatase and rutile) of Titania nanoparticles towards freshwater microalgae: *Chlorella* sp. Aquat Toxicol 161: 154–169
Jain PK, El-Sayed IH, El-Sayed MA (2007) Au nanoparticles target cancer. Nano Today 2:18–29
Jans H, Liu X, Austin L, Maes G, Huo Q (2009) Dynamic light scattering as a powerful tool for gold nanoparticle bioconjugation and biomolecular binding studies. Anal Chem 81:9425–9432
Keel T, Holliday R, Harper T (2010) Gold for good—gold and nanotechnology in the age of innovation. World Gold Counc. 1e20
Khan MS, Vishakante GD, Siddaramaiah H (2013) Gold nanoparticles: a paradigm shift in biomedical applications. Adv Colloid Interf Sci 199-200:44-58
Kim KT, Zaikova T, Hutchison JE, Tanguay RL (2013) Gold nanoparticles disrupt zebrafish eye development and pigmentation. Toxicol Sci 133(2):275–288
Kumar S, Gandhi KS, Kumar R (2006) Modeling of formation of gold nanoparticles by citrate method. Ind Eng Chem Res 46:3128–3136
Kumar A, Boruah BM, Liang XJ (2011) Gold nanoparticles: promising nanomaterials for the diagnosis of cancer and HIV/AIDS. J Nanomater 2011:22
Kumar D, Kumari J, Pakrashi S, Dalai S, Raichur AM, Sastry TP, Mandal AB, Chandrasekaran N, Mukherjee A (2014) Qualitative toxicity assessment of AgNPs on the fresh water bacterial isolates and consortium at low level of exposure concentration. Ecotoxicol Environ Saf 108:152–160
Kumaravel TS, Jha AN (2006) Reliable comet assay measurements for detecting DNA damage induced by ionizing radiation and chemicals. Mutat Res 605:7–16
Lasagna-Reeves C, Gonzalez-Romero D, Barria MA, Olmedo I, Clos A, Ramanujam VMS, Urayama A, Vergara L, Kogan MJ, Soto C (2010) Bioaccumulation and toxicity of gold nanoparticles after repeated administration in mice. Biochem Biophys Res Commun 393: 649–655
Leonard K, Ahmmad B, Okamura H, Kurawaki J (2011) In situ green synthesis of biocompatible ginseng capped gold nanoparticles with remarkable stability. Colloids Surf B: Biointerfaces 82(2): 391–396
Li JJ, Hartono D, Ong CN, Bay BH, Yung LYL (2010) Autophagy and oxidative stress associated with gold nanoparticles. Biomaterials 31: 5996–6003
Manivannan J, Sinha S, Ghosh M, Mukherjee A (2013) Evaluation of multi-endpoint assay to detect genotoxicity and oxidative stress in mice exposed to sodium fluoride. Mutat Res 751:59–65
Mossman T (1983) Rapid colorimetric assay for cellular growth and survival: application to proliferation and cytotoxic assays. J Immunol Methods 65:55–63
Nur Y (2013) Gold nanoparticles: synthesis, characterisation and their effect on *Pseudomonas flourescens*. Doctoral dissertation, University of Birmingham
Organisation for Economic Cooperation and Development (OECD) (2011) Freshwater alga and cyanobacteria, growth inhibition test. OECD Guidelines for the Testing of Chemicals, Test No. 201. OECD Publishing, Paris, France. DOI: 10.1787/9789264069923-en
Osler GHR, Sommerkorn M (2007) Toward a complete soil C and N cycle: incorporating the soil fauna. Ecology 88(7):1611–1621
Pan Y, Neuss S, Leifert A, Fischler M, Wen F, Simon U, Schmid G, Brandau W, Jahnen-Dechent W (2007) Size-dependent cytotoxicity of gold nanoparticles. Small 3:1941–1949
Pillai ZS, Kamat PV (2004) What factors control the size and shape of silver nanoparticles in the citrate ion reduction method? J Phys Chem B 108:945–951
Powers K, Brown S, Krishna V, Wasdo S, Moudgil B, Roberts S (2006) Research strategies for safety evaluation of nanomaterials. Part VI. Characterization of nanoscale particles for toxicological evaluation. Toxicol Sci 90:296–303
Remade J (1990) The cell wall and metal binding. In: Biosorption of heavy metals. CRC Press Boca Raton. 83-92

Renault S, Baudrimont M, Mesmer-Dudons N, Gonzalez P, Mornet S, Brisson A (2008) Impacts of gold nanoparticle exposure on two freshwater species: a phytoplanktonic alga (*Scenedesmus subspicatus*) and a benthic bivalve (*Corbicula fluminea*). Gold Bull 41:116–26

Rohiman A, Anshori I, Surawijaya A, Idris I (2011) Study of colloidal gold synthesis using Turkevich method. AIP Conf Proc 1415:39–42

Römer I, White TA, Baalousha M, Chipman K, Viant MR, Lead JR (2011) Aggregation and dispersion of silver nanoparticles in exposure media for aquatic toxicity tests. J Chromatogr A 1218(27): 4226–4233

Sathishkumar M, Pavagadhi S, Mahadevan A, Balasubramanian R (2014) Biosynthesis of gold nanoparticles and related cytotoxicity evaluation using A549 cells. Ecotoxicol Environ Saf 114:232–40

Sayes CM, Marchione AA, Reed KL, Warheit DB (2007) Comparative pulmonary toxicity assessments of C60 water suspensions in rats: few differences in fullerene toxicity in vivo in contrast to in vitro profiles. Nano Lett 7:2399–2406

Schaechter M, Ingraham JL, Neidhardt FC (2006) Microbe. ASM Press, Washington, DC

Schipper M, Nakayama-Ratchford N, Davis CR, Kam NWS, Chu P, Liu Z, Sun X, Dai H, Gambhir SS (2008) A pilot toxicology study of single-walled carbon nanotubes in a small sample of mice. Nat Nanotechnol 3:216–221

Schulz M, Ma-Hock L, Brill S, Strauss V, Treumann S, Gröters S, Ravenzwaay BV, Landsiedel R (2012) Investigation on the genotoxicity of different sizes of gold nanoparticles administered to the lungs of rats. Mutat Res 745:51–57

Sedlak J, Lindsay RN (1968) Estimation of total protein bound and nonprotein sulphydryl groups in tissue with Ellman reagent. Anal Biochem 25:192–1005

Simpson CA, Salleng KJ, Cliffel DE, Feldheim DL (2013) In vivo toxicity, biodistribution, and clearance of glutathione-coated gold nanoparticles. Nanomedicine 9:257–263

Sokolov K, Follen M, Aaron J, Pavlova I, Malpica A, Lotan R, Richartz-Kortum R (2003) Real-time vital optical imaging of precancer using anti-epidermal growth factor receptor antibodies conjugated to gold nanoparticles. Cancer Res 63:1999–2004

Stankus DP, Lohse SE, Hutchison JE, Nason JA (2011) Interactions between natural organic matter and gold nanoparticles stabilized with different organic capping agents. Environ Sci Technol 45(8):3238–44

Tedesco S, Doyle H, Blasco J, Redmond G, Sheehan D (2010) Oxidative stress and toxicity of gold nanoparticles in *Mytilus edulis*. Aquat Toxicol 100:178–186

Tejamaya M, Römer I, Merrifield RC, Lead JR (2012) Stability of citrate, PVP, and PEG coated silver nanoparticles in ecotoxicology media. Environ Sci Technol 46(13):7011–7

Tice RR, Agurell E, Anderson D, Burlinson B, Hartmann A, Kobayashi H, Miyamae Y, Rojas E, Ryu C, Sasaki YF (2000) Single cell gel/comet assay: guidelines for in vitro and in vivo genetic toxicology testing. Environ Mol Mutagen 35:206–221

Tolaymat TM, El Badawy AM, Genaidy A, Scheckel KG, Luxton TP, Suidan M (2010) An evidence-based environmental perspective of manufactured silver nanoparticle in syntheses and applications: a systematic review and critical appraisal of peer reviewed scientific papers. Sci Total Environ 408(5):999–1006

Turkevich J, Stevenson PC, Hillier J (1953) The formation of colloidal gold. J Phys Chem 57:670

Wang H, Joseph JA (1999) Quantifying cellular oxidative stress by dichlorofluorescein assay using micro plate reader. Free Radic Biol Med 27(5):612–616

Wang S, Lawson R, Ray PC, Yu H (2011) Toxic effects of gold nanoparticles on *Salmonella typhimurium* bacteria. Toxicol Ind Health 27(6):547–554

Wu D, Zhang XD, Liu PX, Zhang LA, Fan FY, Guo ML (2011) Gold nanostructure: fabrication, surface modification, targeting imaging, and enhanced radiotherapy. Curr Nanosci 7:110–118

Yah CS (2013) The toxicity of gold nanoparticles in relation to their physiochemical properties. Biomed Res 24(3):400–413

Yang H, Du L, Tian X, Fan Z, Sun C, Liu Y, Keelan JA, Nie G (2014) Effects of nanoparticle size and gestational age on maternal biodistribution and toxicity of gold nanoparticles in pregnant mice. Toxicol Lett 230:10–18

Zeng S, Cai M, Liang H, Hao J (2012) Size-dependent colorimetric visual detection of melamine in milk at 10 ppb level by citrate-stabilized Au nanoparticles. Anal Methods 4:2499

Zhang G, Yang Z, Lu W, Zhang R, Huang Q, Tian M, Li L, Liang D, Li C (2009) Influence of anchoring ligands and particle size on the colloidal stability and in vivo biodistribution of polyethylene glycol-coated gold nanoparticles in tumor-xenografted mice. Biomaterials 30(10):1928–36

Zhang X, Wu D, Shen X, Liu P, Yang N, Zhao B, Zhang H, Sun Y, Zhang L, Fan F (2011) Size-dependent in vivo toxicity of PEG-coated gold nanoparticles. Int J Nanomedicine 6:2071–2081